IOPscience iopscience.iop.org

Home Search Collections Journals About Contact us My IOPscience

Ionic properties of perovskites derived from topological analysis of their wave function

This article has been downloaded from IOPscience. Please scroll down to see the full text article.

1999 J. Phys.: Condens. Matter 11 6329

(http://iopscience.iop.org/0953-8984/11/33/303)

View the table of contents for this issue, or go to the journal homepage for more

Download details:
IP Address: 171.66.16.220
The article was downloaded on 15/05/2010 at 17:02

Please note that terms and conditions apply.

J. Phys.: Condens. Matter **11** (1999) 6329–6336. Printed in the UK PII: S0953-8984(99)03596-1

Ionic properties of perovskites derived from topological analysis of their wave function

Víctor Luaña, Aurora Costales, A Martín Pendás and L Pueyo

Departamento de Química Física y Analítica, Facultad de Química, Universidad de Oviedo, E-33006-Oviedo, Spain

Received 20 April 1999

Abstract. We present in this work a discussion on the quantitative bonding information that can be deduced from the topological analysis of the crystal wave function of 120 alkali halide perovskites. The formalism, recently presented, is a development of the theory of atoms in molecules of Bader into the domain of crystalline materials. We discuss the shape of the ions and show how the classical picture in terms of slightly deformed spheres is contained in the topological description. The nature of the chemical bond in these systems is depicted by means of graphical representation of the electron density and its Laplacian along the surfaces of the attraction basins. The ionicity of the crystals and the behaviour of the ionic radii are also briefly reviewed.

(Some figures in this article appear in colour in the electronic version; see `www.iop.org`)

1. Introduction

The concept of molecular structure as a collection of atoms linked together by a network of bonds is essential in chemistry, physics, and biology. Its great relevance is firmly based on the force of countless experiments and its success derives, above all, from its capability for organizing empirical information. Remarkably, this concept appears to be unrelated to the postulates of quantum mechanics, in spite of the immensely fruitful absorption of quantum ideas by molecular sciences.

The theory of atoms in molecules (AIM) developed by Bader and collaborators [1–3] has provided, however, a rigorous quantum mechanical foundation for the concept of molecular structure. By means of the analysis of the multielectron molecular wave function, AIM theory gives unambiguous answers to many questions of fundamental character and frequent appearance, such as those of atom size and shape, and ionicity, that otherwise seem to occupy a field alien to the quantum interpretation. The AIM theory does not rely on any approximation, or make use of any experimental information. The quality of its predictions is determined by the quality of the wave function analysed.

AIM theory has been extensively applied to gas-phase molecules. Recently, we have presented [4–6] an analysis of the topological properties of the electron density of crystalline solids based on the AIM framework. When applied to periodic systems, the topological analysis produces a number of very interesting new concepts that can be immediately related to prequantum ideas that dominate the empirical discourse on the crystalline structure. As the AIM theory gives an unambiguous description and numerical values for many of these empirical ideas, it can provide a very suitable route to understanding complicated features of bonding and structure in solids, as it has done in the case of molecules.

0953-8984/99/336329+08$30.00 © 1999 IOP Publishing Ltd

In this work we complement the recent study of the ionic perovskites [5], discussing new results and insights deduced from the AIM approach as regards questions such as those of ionic size, ionic representation, and bonding description. The main idea emerging from this work, in addition to all of those discussed before [4, 5], is that empirical models, like that representing the solid as a collection of slightly deformed spheres with a definite electronic charge, can not only be deduced from the AIM theory but also be related in a continuous and accurate way to the formal descriptions directly emerging from topological analysis. This makes the topological approach particularly appealing. In section 2 we give a brief account of the formalism and previous work and in section 3 we present the results and a discussion.

2. AIM theory for crystals; a brief review

2.1. The elementary building blocks

The topological analysis of atoms and molecules developed by Bader and collaborators [1–3] introduces a partition of the Euclidean space into nonoverlapping regions defined by surfaces of zero flux gradient of the electron density ρ. Determination of these surfaces is accomplished by locating the position and type of the zero-gradient points, the critical points (CP), and the field lines connecting them. CP have associated attraction basins or *loci* of space points whose field lines share the end or start CP. A nucleus plus its basin is identified with an atom. Bonding appears when the two lines emerging from a bond CP have different attractors. The network made of nuclei and their bonds is the molecular graph. When it shows a cycle the system is said to have a ring, which has a ring CP inside the linked nuclei. A set of noncoplanar rings may form a cavity holding a cage CP inside.

For crystals, periodicity introduces some new perspectives:

(a) Space group symmetry restricts the possible positions and types of CPs, as it should. The total number of CPs must obey the Morse relation: $n - b + r - c = 0$, with $n \geqslant 1$, $b \geqslant 3$, $r \geqslant 3$, and $c \geqslant 1$; n, b, r, and c are the numbers of nuclear, bond, ring, and cage CPs.
(b) The concept of primary bundle appears, as the set of trajectories starting at a given minimum and ending at a given maximum. They are the minimum region of space surrounded by zero-flux-gradient surfaces. All primary bundles sharing the same nucleus form its attraction basin. Within these regions, the basic principles of quantum mechanics apply. Furthermore, they are topologically equivalent to convex polyhedra of which the cage points are vertices, the bond points are faces, and the ring points are edges. The nucleus plus its attraction basin is identified as the atomic shape.
(c) The attraction basins must be finite and the atomic volume can be unambiguously defined.

The problem of finding the CPs is far from trivial. Extensive analysis and software development has been completed in our group [6] to make this problem tractable.

2.2. The classification scheme

The rich topological information contained in the electronic density can be clarified by means of taxonomic instruments that permit a hierarchical organization of the crystal under consideration. In the case of the 120 AMX_3 perovskites discussed in [5] (A = Li, Na, K, Rb, Cs; M = Be, Mg, Ca, Sr, Ba, Zn; X = F, Cl, Br, I), the following classification scheme has been useful.

The special positions of the $Pm\bar{3}m$ group 1a, 1b, 3c, and 3d must be CPs. Only the 3c position is not occupied by crystal ions. The type of CP at this point is the first taxonomic

criterion, introducing the concept of topological family. The assignment is as follows. Families will be called $\mathcal{B}$, $\mathcal{R}$, $\mathcal{C}$ if the CP at 3c is a bond, ring, or cage point, respectively. A family contains many crystals: 2 in $\mathcal{B}$, 48 in $\mathcal{C}$, 70 in $\mathcal{R}$. Further organization is gained through a second classification criterion: the total number of different-symmetry CPs, $\tau = \tau_n + \tau_b + \tau_r + \tau_c$, where the τ_i are the total numbers of different CPs of each type. This second level gives the topological species. The $\mathcal{B}$ family has only one species, the $\mathcal{B}_{10}$. The $\mathcal{C}$ and $\mathcal{R}$ families each have three: $\mathcal{C}_8$, $\mathcal{C}_{10}$, $\mathcal{C}_{12}$ and $\mathcal{R}_9$, $\mathcal{R}_{11}$, $\mathcal{R}_{13}$. This makes a total of seven topological species with the following distribution of crystals among them: $\mathcal{B}_{10}(2)$, $\mathcal{C}_8(21)$, $\mathcal{C}_{10}(15)$, $\mathcal{C}_{12}(12)$, $\mathcal{R}_9(27)$, $\mathcal{R}_{11}(25)$, $\mathcal{R}_{13}(18)$. An inverse relation between topological complexity of the species (τ-number) and their crystal occupation is immediately observed. Notice the surprising complexity in the topology of the density of these 120 crystallographically analogous crystals.

The organizing power of a topological classification like this has a counterpart in geometrical quantities like the ionic radii, thus representing a promising instrument for discovery. The $\mathcal{B}$ family contains three different bonds: b_1 (M–X), b_2 (A–X), and b_4 (A–A). The $\mathcal{C}$ and $\mathcal{R}$ families do not have A–A bonds. They have b_1, b_2, and b_3 (X–X) bonds. Thus, only the two members of the $\mathcal{B}$ family, $CsSrF_3$ and $CsBaF_3$, have A–A bonds.

2.3. The graphical representation

In simple molecules, the arrangement of the CPs and their connecting lines creates the molecular graph, which immediately depicts the familiar image of the molecule. For solids, depicting this graph is a nontrivial task, given the huge number of CPs in the unit cell (up to 104 in the $\mathcal{R}_{13}$ family). A much more feasible and charming alternative is to three-dimensionally depict the attraction basin for each ion. A basin has no CPs inside, apart from its nuclear point. All other CPs lie at the 2D boundaries. We can associate with these CPs a polyhedron: cage points becoming vertices, bond points faces, and ring points edges. In this way, we can approximate the attraction basins by polyhedra.

Now we can see the difference between the classical view of the atomic building of a crystal, in terms of slightly deformed spheres, and the topological visualization of the atomic regions. The conceptual model of classical spheres has two salient features:

(a) it strongly suggests the existence of isotropic atomic radii, and

(b) the spheres do not fill the entire space.

The first feature lies at the root of the well-known difficulty of organizing crystal arrangements by means of empirical radii. The second one produces interstitial spaces that remain explicitly out of the picture. Again this limitation appears many times, as in the muffin-tin approximation.

The topological approach does not suffer from these two deficiencies. Attraction basins give different radii for different directions and fill the entire space. Some striking consequences of this filling have been discussed before [5], as the appearance of spectacular wings in the fluoride basins of $LiCaF_3$.

In figure 1 we show the ionic basins of $KCaF_3$, a crystal of the $\mathcal{C}_8$ species. Here the fluoride basin shows remarkably the spikes needed to fill the space without forming F–F bonds. More complex topological species, containing X–X bonds, have less demanding requirements and show basins that have round, nearly spherical shapes. As a notable consequence, the more complex topological species show simpler, more familiar 3D representations of the ionic basins, whereas the striking geometrical forms appear in the simplest topological species.

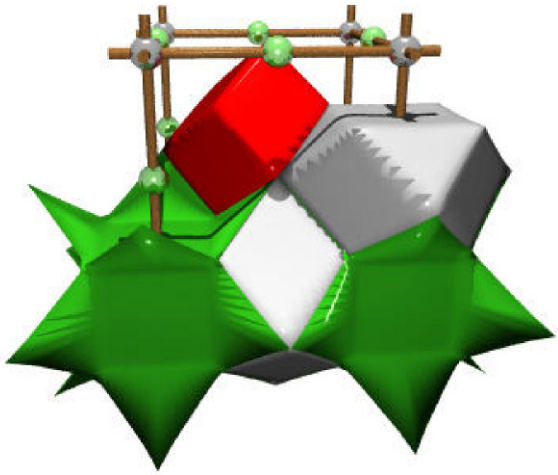

Figure 1. Ionic basins for $KCaF_3$ computed with the program CRITIC and rendered with POV-Ray [12].

2.4. Topology and geometry

We finally recall that this topological diversity has a geometrical counterpart. It has been discussed elsewhere [5]. We simply notice here that the topological analysis allows a direct estimation of ionic radii, along different bond directions, as the distance from the nucleus to the surface of its basin. So, b_1 (M–X) CPs give the cationic radius R_M and the anionic radius R_{1X}, b_2 (A–X) gives R_A and R_{2X}, and b_3 (X–X) gives R_{3X}. The very remarkable result is that the quantities $\xi = R_M/R_{1X}$ and $\eta = R_A/R_{2X}$ define a plane that completely determines the topological species of the crystal. If $\eta \geqslant 0.88$, the crystal belongs to the $\mathcal{C}$ family; otherwise it belongs to the $\mathcal{R}$ family. Also, the topological complexity decreases when ξ increases. No empirical scheme of atomic radii has shown such an accurate classification strength.

3. Quantitative bonding information derived from the electronic density

We now discuss results obtained from the analysis of the crystal wave function computed for these 120 perovskites with the *ab initio* perturbed-ion method [7, 8] at the theoretically determined equilibrium geometries. Exponential basis sets of Clementi and Roetti [9] have been used for all cases and the unrelaxed hard Coulomb hole formalism of Clementi [10] has been adopted for estimating the correlation energy.

We will briefly discuss some examples that show the wealth of quantitative information that can be obtained from the topological analysis of the electron density. Relevant bonding information appears from appropriate manipulation of the density itself, as well as from related scalar fields. Furthermore, quantitative information emerges from the fact that attraction basins are regions of space in which the laws of quantum mechanics hold. Thus, we can extract the required information by direct integration of appropriate quantum mechanical operators over the electron density [11].

Details of the accurate numerical quadratures required to accomplish this goal have been given elsewhere [5]. Accuracies better than 0.01 $Å^3$ in the cell volume and better than 0.001 au in electronic charge have been achieved in these perovskites.

3.1. What is the shape of the ions?

We have seen above that the topological partition of the crystal completely fills the space and that the atomic shapes are assigned to convex polyhedra. We have remarked the contrast between this view and the classical representation of ionic solids in terms of slightly deformed spheres that leave unfilled interstitial space. We will show now that the topological description contains this representation too. This is so because the electron density is a scalar field with extremely large variations along the bonding lines. As an example, we notice that in $KMgF_3$ the density at the nuclei is 4.539×10^3 (K^+), 1.091×10^3 (Mg^{2+}), and 3.369×10^2 (F^-) au, whereas it becomes 3.661×10^{-2} au at the Mg–F bond CP, 1.177×10^{-2} au at the K–F bond CP, and 9.913×10^{-3} au at the F–F bond CP.

The shape of the ions, as deduced from isodensity contours, heavily depends on the value selected for drawing the isosurface. In this example, any representation with $\rho \geqslant 0.040$ au would mask any bonding feature and will give the classical view of nonoverlapping spheres centred at the nuclei. As we reduce the value of the selected density and approach the bonding regime, the ionic species develop small spikes in the directions of the bond lines. The spikes of two ions touch when the isodensity coincides with the density of the bond CP. The surfaces of lower density show the spikes transformed in bonding spaces of approximately cylindrical shape. In figure 2 we present the surfaces of constant density for $KMgF_3$ for $\rho = 0.020$ au. This value is low enough to reveal the Mg–F bond but still leaves the K^+ ion as a nearly perfect isolated sphere. The shape of the ions and the bonding picture of a crystal are thus at hand from the results of the topological analysis, The electron density, properly scanned, can give extremely detailed information of quantitative value and great beauty.

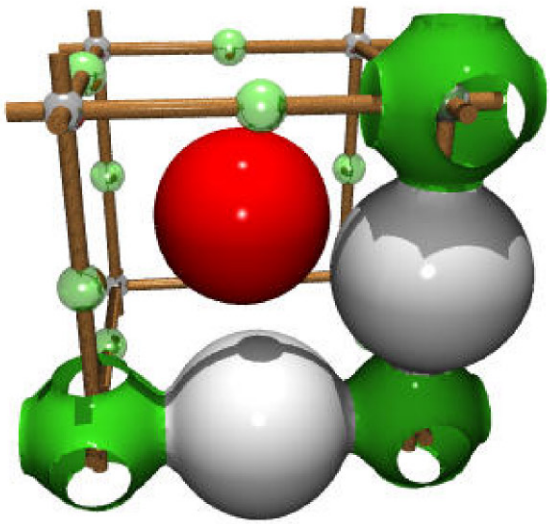

Figure 2. Surfaces of constant electron density $\rho = 0.020$ au in $KMgF_3$ computed with the program CRITIC and rendered with POV-Ray [12].

3.2. The nature of the bond

The topological analysis is particularly well suited to provide information on the nature of the chemical bond in crystals because the graphical representation of appropriate scalar fields on the surfaces of the basins gives illuminating images of the bonding situation. Thus, depicting

directly the electron density we observe the zones of accumulation and depletion of charge. Sites where electron density heaps up reveal the presence of bond CPs. In figure 3 (left) we show the electron density on the surfaces of the basins for $CsBeI_3$, a crystal of the $\mathcal{C}_{12}$ topological species. We observe that the accumulation of density along the I–I bond is larger than those along the Be–I and Cs–I bonds.

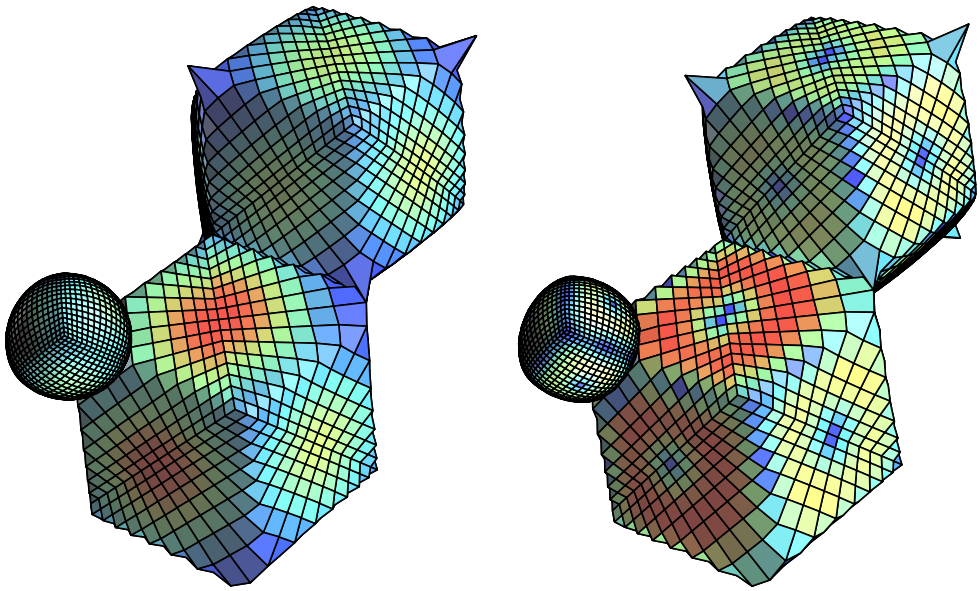

Figure 3. The electron density (left) and Laplacian (right) on the surface of the ionic basins of $CsBeI_3$ computed with the program CRITIC and rendered with GEOMVIEW [13]. Higher values correspond to darker tone.

The strength of the bond, however, is determined by the behaviour of the Laplacian of the electron density, $-\nabla^2\rho$. A representation of this scalar field for $CsBeI_3$ appears in figure 3 (right). Here we see that the larger accumulation appears along the Be–I directions, showing the relevance of this bond in the formation of the perovskite. This behaviour of ρ and $-\nabla^2\rho$ on the basin surfaces has been observed in the 120 cases. Other scalar fields and regulatory theorems like the virial theorem can be analysed in a similar way.

3.3. Ionicity and ionic radius

We finally describe the direct way of analysing bonding properties like ionicity (through the ionic topological charges) and ionic radii. The ionic charge is obtained by integration of the charge operator over the density of the basin. Topological ionic charges obtained in this way, averaged over the 120 perovskites, are collected in table 1.

We see that the charges of the alkali ions deviate by 0.01 au from the formal +1.0 value, revealing the high ionicity of these crystals and the negligible contribution of the mono-positive A species to the rearrangement of charge accompanying the process of crystal formation. The gross average for the halide ions is -0.952 au and that for the di-positive cations is 1.863 au. Thus, the image of a weak $X \rightarrow M$ charge transfer emerges, in accordance with the qualitative expectations from conventional bonding descriptions. The amount of this effective charge transfer correlates with the nuclear charge in the M^{2+} series but this correlation is not apparent

Table 1. Topological ionic charges averaged over 120 perovskites. The last line gives gross average values.

Ion	Charge	Ion	Charge	Ion	Charge
Be	1.954	Li	0.9970	F	−0.9630
Mg	1.891	Na	0.9914	Cl	−0.9446
Ca	1.863	K	0.9896	Br	−0.9490
Sr	1.832	Rb	0.9852	I	−0.9499
Ba	1.826	Cs	0.9990		
Zn	1.811				
$\langle q_M \rangle$	1.863	$\langle q_A \rangle$	0.992	$\langle q_X \rangle$	−0.952

within the X^- and A^+ series.

Let us turn now to the concept of ionic radius. As remarked above, the ionic radius assigned to an attraction basin depends on the direction selected. A single value can be assigned to an ion by averaging over all directions. This average can be defined as the radius of the sphere of volume equal to that of the ionic basin. The resulting values behave in complete agreement with the physical expectations. For instance, they increase, for each group of ions, with the atomic number; they show larger dispersion when going down the Periodic Table, etc. It has been noticed [5] that the alkali halides show a larger variation over the crystals, in contrast with their smaller polarizability. This dispersion can be related to the weaker bond holding these species, in agreement with the picture produced by their almost nominal electronic charge.

From all of this and previous [4, 5] discussions we conclude that the AIM theory supplies a rigorous foundation for important historical concepts like ionicity, index of coordination, coordination polyhedra, or volume of an atom or ion in a solid. Several interesting mappings between atoms and polyhedra can be built, some of which have been examined and exploited in this work. We believe that there is plenty of room in solid-state thinking for the new tools and concepts emerging from the AIM approach. A judicious use of them will give new ways to establish an accurate correlation of quantum mechanical origin between the chemical behaviour and chemical structure in solids. This new approach should offer a new path to insight and discovery.

Acknowledgments

Financial support was provided by the Spanish Dirección General de Investigación Científica y Técnica (DGICYT), Project No PB96-0559.

References

[1] Bader R F W, Nguyen-Dang T T and Tal Y 1981 *Rep. Prog. Phys.* **44** 893
[2] Bader R F W 1990 *Atoms in Molecules: a Quantum Theory* (Oxford: Oxford University Press)
[3] Bader R F W *Theory of Atoms in Molecules* `http://www.chemistry.mcmaster.ca/faculty/bader/aim`
[4] Martín Pendás A, Costales A and Luaña V 1997 *Phys. Rev.* B **55** 4275
[5] Luaña V, Costales A and Martín Pendás A 1997 *Phys. Rev.* B **55** 4285
[6] Martín Pendás A 1995 *The CRITIC Program* University of Ovieko
[7] Luaña V and Pueyo L 1990 *Phys. Rev.* B **41** 3800
[8] Blanco M A, Luaña V and Martín Pendás A 1997 *Comput. Phys. Commun.* **103** 287
[9] Clementi E and Roetti C 1974 *At. Data Nucl. Data Tables* **14** 177
[10] Chakravorty S J and Clementi E 1989 *Phys. Rev.* A **39** 2290
[11] Bader R F W 1994 *Phys. Rev.* B **49** 13 348

[12] *POV-Ray: Persistence of the Vision Ray Tracer* version 2.2 (1994) was devised by C Young *et al*. It can be obtained through anonymous ftp at `ftp.povray.org`. See also the POV-Ray WWW home page.

[13] *GEOMVIEW* (1995) was devised by M Phillips, T Munzner and S Levy; it is available via anonymous ftp from `geom.umn.edu`. Have a look at the home page of the Geometry Center at the University of Minnesota.